PHYSICAL REVIEW E

STATISTICAL PHYSICS, PLASMAS, FLUIDS, AND RELATED INTERDISCIPLINARY TOPICS

THIRD SERIES, VOLUME 54, NUMBER 4 PART B OCTOBER 1996

ARTICLES

Wetting description of block copolymer thin films

Scott T. Milner
Exxon Research & Engineering, Route 22 East, Annandale New Jersey 08801

David C. Morse
Materials Research Laboratory, University of California, Santa Barbara, California 93106

(Received 18 October 1995)

Symmetric diblock copolymers undergo a weakly first-order microphase separation transition to a lamellar phase. In a thin film of thickness d this transition is altered for two reasons: the film geometry imposes commensurability restrictions on the concentration profiles, and the surface field favors one of the two blocks. The latter effect dominates for $d>\xi$, where ξ is the correlation length near T_c. We construct a wetting Hamiltonian, in which the slowly varying amplitude $\psi(z)$ of the composition $c(z)=2\psi(z)\cos(q_0 z)$ is the order parameter, and explore the changes in the profile induced by changes in temperature, surface field, and d/ξ. The resulting phase diagram exhibits a line of first-order prewetting transitions ending in a critical point, and a capillary condensation transition to an ordered film. Turning to commensurability effects, we compute the ranges of thickness near half-integer numbers of layers for which the free surface of a copolymer film is unstable to capillary waves, analogous to spinodal decomposition in two dimensions. [S1063-651X(96)01409-2]

PACS number(s): 61.41.+e, 61.30.Cz, 81.30.−t, 68.55.−a

I. INTRODUCTION

The isotropic-lamellar transition in diblock copolymer melts has received considerable attention, both experimental and theoretical, for two contradictory reasons. First, because the lamellar phase seems at first sight the simplest possible ordered mesophase and, second, because in fact the transition is an unusual fluctuation-induced first-order transition, and the ordered lamellar phase has all the richness with respect to elasticity and dynamics of smectic liquid crystals, of which lamellar phases are an example.

In this paper we are concerned with the ways in which the behavior of diblock copolymer melts confined to a thin film differs from the behavior of bulk samples. We may consider films of a few layers or many layers in thickness, above or below the bulk ordering transition, thick or thin with respect to the correlation length, with or without surface fields that prefer one of the two blocks of the diblock copolymer. We may consider films of commensurate or incommensurate thickness with respect to the lamellar order, and films confined between two substrates or with a free surface.

These various cases are of interest because of the great variety of possible ways a diblock melt might respond to confinement into a thin film. All these phenomena can be directly observed with reflectivity techniques, which have been used extensively to study such copolymer films [1–5]. Some of the phenomena we shall describe have been observed experimentally, and some have yet to be observed but surely must be present. We have tried to be imaginative with regard to the behavior of lamellar films, but the films are likely to be yet more resourceful.

Confinement of a diblock melt into a thin film has two basic effects. The film boundaries inevitably impose some surface field on the monomer concentration difference $c(r)=c_A(r)-c_B(r)$. Also, the finite film thickness imposes commensurability on the film if it is to order with lamellae parallel to the film, as is favored by the presence of any surface field. Many of the effects of surface fields and incommensurability on a thin film of a lamellar (or smectic) fluid have been considered previously in Refs. [6–8]. Such a film responds in several ways to these intrusions. At temperatures above the temperature of the first-order ordering transition temperature, surface fields induce some lamellar order at the boundaries, which may penetrate across the film if $\xi \gtrsim d$, where ξ is the correlation length for the decay of oscillatory composition variations and d is the thickness of

the film. If the film thickness is incommensurate with the period of the bulk lamellar phase, and order does extend across the film, then the film may either order at a nonoptimal wave number, which depresses the temperature of the first-order transition, or may undergo a capillary-wave instability toward a state with an inhomogeneous film thickness. The latter phenomenon is analogous to spinodal decomposition in two dimensions, with the thickness $d(\vec{x})$ of the film playing the role of a conserved order parameter analogous to the composition in a demixing binary fluid. At temperatures near that of the bulk ordering transition, a small surface field may have large effects, producing lamellar ordering at the surface of an amplitude comparable to that of the bulk-ordered state. Because the isotropic-smectic transition is first order, a small surface field may also, in a phenomena analogous to capillary condensation of a confined binary fluid mixture, [9] induce order throughout a film of thickness $d \gg \xi$ at a transition temperature above that of the bulk transition.

This paper, which considers both surface field and commensurability effects in various regimes, is organized as follows. In Sec. II, the basic results of the Brazovskii-Fredrickson-Helfand theory of the bulk isotropic-lamellar transition are reviewed. We show that the resulting bulk free energy is very well approximated by an even, sixth-order polynomial in the concentration difference $c(r)$, similiar to that used previously by Fredrickson and Binder, [10] which greatly simplifies the rest of our calculations.

In Sec. III, we compute the composition profile and free energy of a thin film within a linear response approximation appropriate to describing surface-induced order at temperatures well above the bulk transition temperature. In this weakly ordered regime, it is possible to calculate the profile and free energy for any value of d/ξ. The effects of commensurability result in a free energy that is an oscillating function of thickness d, such that thin films near a half-integer number of layers can be unstable to the growth of capillary waves.

In Sec. IV, we develop an approach to lamellar phases in thin-film geometries based on writing the concentration variable $c(r)$ as a slowly varying amplitude $\psi(r)$ times a cosine wave with a slowly varying phase $\phi(r)$, and performing a gradient expansion of the Brazovskii-Fredrickson-Helfand free energy. This approach allows us to examine the formation of strong order (i.e., order of magnitude comparable to that found in the bulk state near the bulk transition temperature) in any system in which both d and ξ are significantly larger than the bulk lamellar spacing. We check this approach first with a reexamination of the linear response regime. The simplest case beyond linear response is that of a strongly correlated film, with $\xi \gg d$, and no surface field, for which the amplitude $\psi(r)$ is essentially uniform across the film. Then the phase variable must ''stretch'' the wave number away from the preferred value to make the layering commensurate with the film thickness. This results in an oscillating dependence of the ordering transition temperature on thickness, as well as bands of thickness near half-integer values that are again unstable to capillary waves.

In Sec. V, we develop analogies to prewetting phenomena predicted by Cahn. Our gradient-expansion free energy reduces to a form similar to that of a binary fluid mixture, a squared-gradient term plus a double-well potential, if the spatial variation of the phase variable is neglected, which is shown to be a reasonable approximation for any commensurate film. A film of thickness $d \gg \xi$ will undergo a first-order transition between a ''disordered'' state in which induced lamellar order exists only near the walls and an ''ordered'' state in which lamellar order of magnitude similar to that of the bulk ordered state extends throughout the film. Depending on the strength of the surface field, the amplitude $\psi(z)$ near either boundary at temperatures infinitesimally above this ordering temperature may be in one of two states: ''nonwet,'' or ''wet:'' In the nonwet state, the amplitude of induced lamellar order is smaller than that in the bulk ordered state and decays away within a bulk correlation length of the boundary. In the wet state, the amplitude of induced lamellar order at the boundaries exceeds the amplitude of the bulk ordered state, and may persist a greater distance into the film. In a semi-infinite film, the thickness of this wetting layer of lamellar order diverges as the transition temperature is approached from above. At temperatures above the order-disorder transition temperature, these two states are separated in the (h_s, t) plane by a line of first-order prewetting transitions, which terminates in a critical end point. In a film of finite thickness, the wetting layers on the opposite boundaries may jump together discontinuously at a temperature above that of the bulk transition. This shifting of the transition temperature, which is analogous to capillary condensation, occurs when the free energy cost of ordering the remaining material in the center of the film is less than the cost of the two interfaces between surface-ordered material and the disordered center.

In Sec. VI, we present some final remarks, areas for further work, and suggestions for future experiments. Details of the exact linear-response calculations, and the gradient expansion of the Brazovskii free energy, are presented in Appendices A and B, respectively.

II. ISOTROPIC-LAMELLAR TRANSITION

A. Brazovskii model

The isotropic-lamellar transition in diblock copolymers has been analyzed theoretically by Brazovskii, [11] Leibler, [12] and Fredrickson and Helfand [13]. Leibler developed and analyzed the mean-field theory of a melt of diblock copolymers, which in the case of symmetric diblocks takes the form

$$\beta H_{\text{Leibler}} = \frac{1}{2}\int \frac{d^3q}{(2\pi)^3 \nu}\Gamma_2(q)\Phi(q)\Phi(-q) + \frac{\Gamma_4}{4!\,\nu}\int d^3r[\Phi(r)]^4, \tag{1}$$

plus higher order terms whose effects are unimportant at temperatures very near the transition temperature. Here $\Phi(r)$ is the volume fraction of one of the two monomer species and ν is a monomeric volume. The quadratic coefficient $\Gamma_2(q) \equiv S^{-1}(q) = S_0^{-1}(q) - 2\chi$ is the random phase approximation (RPA) inverse structure factor. The ideal $(\chi = 0)$ inverse structure factor $S_0^{-1}(q)$ can be approximated near its minimum by

$$S_0^{-1}(q) \simeq \frac{1}{N}[20.99 + 0.1481(x - x_0)^2], x \equiv q^2 R^2/6,$$
$$x_0 = 3.785, \tag{2}$$

where R^2 is the mean-square end-to-end distance of the copolymer. The quartic term is approximated here by a local interaction, in which $\Gamma_4 = \Gamma_4(\vec{q}_0, -\vec{q}_0, \vec{q}_0, -\vec{q}_0) \simeq 156.56/N$ denotes the value of the nonlocal quartic coupling appropriate to bulk lamellar order at the preferred wave number.

Fredrickson and Helfand [13] put this effective Hamiltonian in the form of the effective Hamiltonian introduced by Brazovskii,

$$H_{\text{eff}} = \frac{1}{2}\int dq[\tau + (q - q_0)^2]c(q)c(-q) + \frac{\lambda}{4!}\int dr[c(r)]^4. \tag{3}$$

For symmetric diblock copolymers, the various coefficients are related to molecular parameters by [13]

$$\tau = 1.647(N\chi_c - N\chi)/\overline{N},$$
$$N\chi_c = 10.495,$$
$$q_0^2 = 22.71/\overline{N}, \tag{4}$$
$$\lambda = 106.18/\overline{N},$$
$$c(x) = 1.102\Phi(x)$$

and all lengths are to be measured in terms of the microscopic ''packing length'' $l_p \equiv (N\nu)/R^2$, a length-independent parameter that is the ratio of the displaced volume of a chain $N\nu$ and the mean-square end-to-end distance. The quantity $\overline{N} \equiv R^6/(N\nu)^2$ is a measure of chain molecular weight. The quantity τ varies linearly with χ (which decreases with increasing temperature) and may be assumed to increase linearly with increasing temperature over the small range of temperatures near the transition temperature upon which we will focus. This quantity will thus be used in what follows as a measure of reduced temperature.

This effective Hamiltonian describes the lamellar ordering of a scalar field $c(r)$ at a finite preferred wave number q_0, without preference for the direction of the lamellar normals. Because of this degeneracy in layering direction, a mean-field treatment of Eq. (3) goes disastrously wrong, in the following way: neglecting the nonlinear interaction through the quartic term of independent lamellar fluctuations, the mean-square fluctuation of concentration at a point in space diverges as $\tau \to 0$,

$$\langle c^2(0)\rangle = \int \frac{dq}{\tau + (q - q_0)^2} \approx \frac{q_0^2}{2\pi\tau^{1/2}}. \tag{5}$$

Since $c(r)$ must remain finite, the different lamellar fluctuations must compete strongly through the quartic term as $\tau \to 0$, no matter how small λ is. Brazovskii showed that the leading behavior for small λ was captured by the use of a self-consistent Hartree approximation, which is equivalent [14] to approximating the probability distribution for $c(q)$ by a Gaussian, with statistical weights determined by applying the variational theorem.

The inverse susceptibility obtained in this approximation is, for both ordered or disordered states, of the form

$$g^{-1}(q) \equiv \langle \delta c(q)\, \delta c(-q)\rangle^{-1} = r + (q - q_0)^2, \tag{6}$$

where $\delta c(q) \equiv c(q) - \langle c(q)\rangle$. The self-consistent equations for r and for the bulk free-energy density f_B and its derivative $h = (1/2)\partial f/\partial a$ are

$$r = \tau + \alpha\lambda/\sqrt{r} + \lambda a^2,$$
$$h = \tau a + \alpha\lambda a/\sqrt{r} + \lambda a^3/2, \tag{7}$$
$$f_B = 2\alpha\sqrt{r} - \alpha^2\lambda/(2r) + \tau a^2 + \lambda a^4/4.$$

Here a is the amplitude of the assumed periodic order, $\langle c(r)\rangle = 2a\cos(q_0 z)$, h is a field conjugate to a, and $\alpha \equiv q_0^2/(4\pi)$.

B. Scaling behavior

When r, ψ, and f_B are given in terms of the characteristic units

$$r^* \equiv (\lambda\alpha)^{2/3},$$
$$(a^*)^2 \equiv (r^*/\lambda) = \alpha^{2/3}\lambda^{-1/3}, \tag{8}$$
$$f^* \equiv r^*(a^*)^2 = \alpha^{4/3}\lambda^{1/3},$$

the self-consistent equations are of the same form as those given in Eqs. (7), but with λ and α replaced by unity. Thus the results in the scaled variables $\tilde{r} = r/r^*$, $\tilde{a} = a/a^*$, and $\tilde{f} = f/f^*$ are ''universal'' in the sense that they do not depend on how nearly second order the transition is.

To compute the free energy density $f(\tau, a)$, one may solve the first of Eqs. (7) for $r(\tau, a)$, and substitute into the last of Eqs. (7). The resulting free energy develops a second minimum for τ less than the spinodal temperature τ_s, and undergoes a first-order transition at τ_c, with the amplitude a jumping to a finite value a_c. Numerical calculations give the results

$$\tau_s = -1.889 r^*, \quad r_{\text{dis}}(\tau_s) = 0.224 r^*, \quad r_{\text{ord}}(\tau_s) = 0.630 r^*,$$
$$\tau_c = -2.031 r^*, \quad r_{\text{dis}}(\tau_c) = 0.201 r^*, \quad r_{\text{ord}}(\tau_s) = 1.058 r^*, \tag{9}$$
$$a_c = 1.455 a^*.$$

For a given value of copolymer chain length N and hence λ, the various quantities associated with the first-order transition are determined. From the mapping from the Leibler Hamiltonian to the Brazovskii Hamiltonian, the following results are obtained [13]:

$$r^* = 33.24\overline{N}^{-4/3},$$
$$(a^*)^2 = 0.313\overline{N}^{-1/3}. \tag{10}$$

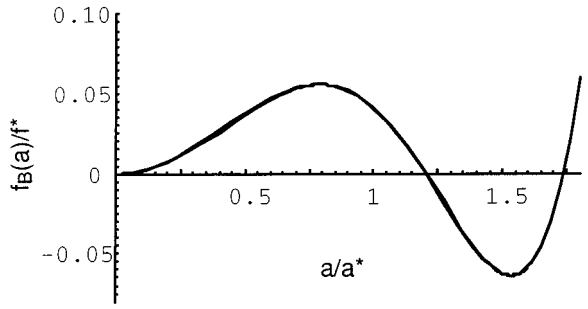

FIG. 1. The Brazovskii free energy (shown here in the reduced units defined in Sec. II B) is very closely approximated by a cubic polynomial in a^2, with coefficients that vary linearly with τ through the relevant range of temperatures between τ_s and τ_c.

Note that in the limit of long copolymer chains, the amplitude of order at the transition vanishes as $N^{-1/3}$. This is the measure of deviation from mean-field behavior; since the relevant scale for τ is $\chi_{\rm mf}=10.495/N$, the relative size of the non-mean-field region in χ (or temperature) is

$$(\chi_c-\chi_s)/\chi_{\rm mf}=0.272\overline{N}^{-1/3}. \tag{11}$$

A particularly useful way of characterizing the degree of first-order behavior is in terms of $(q_0\xi^*)^2\equiv q_0^2/r^*$, the characteristic correlation length $\xi^*\equiv 1/\sqrt{r^*}$ at the transition in units of the layer spacing. [From Eq. (6) we see that r has the interpretation of ξ^{-2}, where ξ is a fluctuation renormalized correlation length.] From Eqs. (10) and (4) we find

$$(q_0\xi^*)^2=0.683\overline{N}^{1/3}. \tag{12}$$

Thus $q_0\xi^*$ becomes large in the limit of large $\overline{N}$, which implies nearly second-order behavior at the transition. For a typical copolymer one might have $\overline{N}$ on the order of 10^4 and hence $(q_0\xi^*)^2\approx 15$, i.e., a characteristic correlation length ξ^* of about 0.61 in units of the lamellar period $l=2\pi/q_0$. At the transition, the disordered state correlation length is $\xi_{\rm dis}\equiv[r_{\rm dis}(\tau_c)/r^*]^{-1/2}\xi^*$, which is $0.201^{-1/2}=2.23$ times larger.

C. Polynomial fit to $f_B(a)$

It is convenient to have an approximate form for the Brazovskii free energy that is more explicit than the solution of the nonlinear equations Eqs. (7). We might hope to represent $f_B(\psi)$ as a polynomial in ψ, with coefficients depending linearly on the effective temperature τ near the transition. Since the Hamiltonian is invariant under the symmetry $c(r)\to -c(r)$ or equivalently $a\to -a$, one might expect the following polynomial approximation to be a sensible starting point:

$$f_B(a)\approx f_p(a)=c_1a^2-c_2a^4+c_3a^6. \tag{13}$$

Evidently, $f_p(a)$ has a minimum at $a=0$ with the value $f_p(0)=0$, corresponding to the disordered state. The three coefficients c_i can be chosen so that $f_p(a)$ has a second minimum at the correct ordered-state amplitude $a=a_c$ with the correct value $f_B(a_c)$, and a maximum with the correct value $f_B(a_m)$ at some lesser amplitude $a=a_m$ to be adjusted. Surprisingly, this procedure gives a very close fit to the numerically evaluated Brazovskii free energy throughout the interesting range of temperatures and amplitudes. A typical fit is shown in Fig. 1. In fact, in the vicinity of the transition the following expressions suffice for the $\{c_i\}$:

$$\begin{aligned} c_1&=0.441[1+0.752(\tau+\tau_c)]/a_c^2,\\ c_2&=0.441[-2+0.910(\tau+\tau_c)]/a_c^4,\\ c_3&=0.441[1+0.332(\tau+\tau_c)]/a_c^6, \end{aligned} \tag{14}$$

where $\tau_c=-2.0305$ and $a_c=1.445$ are the transition temperature and the amplitude at the transition. Note that at $\tau=\tau_c$, we have $f_p(a)=0.441(a/a_c)^2[1-(a/a_c)^2]^2$, which clearly shows the double minima at $a=0$ and $a=a_c$. A sixth-order polynomial approximation with slightly different coefficients has been used previously by Fredrickson and Binder [10].

III. LINEAR RESPONSE

In this section we use a linear-response approximation to describe the formation of weak surface-field-induced order at temperatures above the bulk transition temperature. For this purpose, we expand the concentration field in terms of normalized cosines

$$\begin{aligned} c(x,z)&=\frac{1}{Ad}\sum_{m,k_\perp} c(m,k_\perp)f_{m,k_\perp}(x,z),\\ f_{m,k_\perp}(x,z)&\equiv\sqrt{2}\exp(i\vec{k}_\perp\cdot\vec{x})\cos(\pi mz/d). \end{aligned} \tag{15}$$

Here the sum over m runs over the positive integers, and $\vec{x}$ and $\vec{k}_\perp$ represent vectors in the x-y plane. The expansion in cosines automatically satisfies both the requirement that the concentration field have zero integral (symmetric diblocks having no excess of either type of monomer), as well as the reflecting boundary condition appropriate to melts confined between surfaces.

The Brazovskii free energy to quadratic order in c is of the form:

$$F=\frac{1}{2Ad}\sum_{m,k_\perp} g^{-1}(m,k_\perp)c(m,k_\perp)c(m,-k_\perp), \tag{16}$$

where $g(m,k_\perp)$ denotes the value of the bulk structure factor of Eq. (6) evaluated at a wave vector $q=k_\perp+\hat{z}k_m$, with $k_\parallel=\pi m/d$.

We write the structure factor here in a slightly more elaborate form:

$$\begin{aligned} g(m,k_\perp)&=\frac{4q^2}{4q_0^2r+(q^2-q_0^2)^2},\quad q^2\equiv k_\perp^2+k_m^2,\\ k_m&\equiv\pi m/d. \end{aligned} \tag{17}$$

This reduces to the Brazovskii expression $g(q)=[r+(q-q_0)^2]^{-1}$ near $q=q_0$, but has two important properties missing from that simple expression: (1) it is a function of q^2, not of $|q|$, the analyticity of which makes

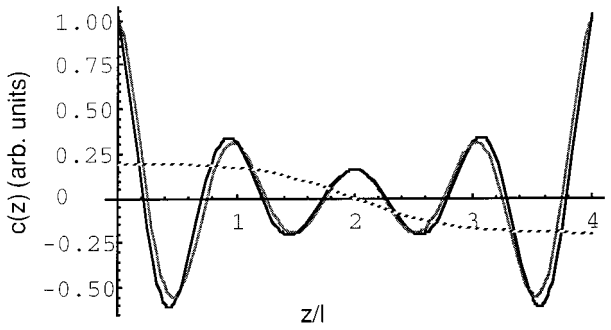

FIG. 2. Linear-response concentration profile for a film of thickness d, with $d/l=4$ ($l=2\pi/d$ the lamellar period) and $q_0\xi^*=5$. The shaded curve is the approximate profile neglecting phase variations, and the dashed curve is the phase variation.

subsequent arithmetic nicer; and (2) it vanishes as q tends to zero, which guarantees that there is no long-wavelength concentration variation (impossible in a symmetric diblock copolymer). It has been pointed out by several authors [15,16] that using an inverse structure factor of the form $g^{-1}(q)=Aq^{-2}+Bq^2+C$, which is equivalent to that given above, also captures the correct algebraic forms of the RPA structure factor in the limits of very high and very low q and yields a rather good fit to the full structure function over the entire range of q. Here, because we focus on behavior near the critical temperature, where the composition field is dominated by Fourier modes with $q\simeq q_0$, we fix the coefficients A, B, and C so as to give exactly the desired position q_0 for the minimum of $g^{-1}(q)$, and for the value and second derivative with respect to q of $g^{-1}(q)$ at its minimum.

Coupling to surface fields takes the form

$$F_{\text{surface}}=-\int d^2x[c(x,0)h_l+c(x,d)h_r], \tag{18}$$

which becomes upon Fourier expansion

$$F_{\text{surface}}=-\frac{\sqrt{2}}{d}\sum_m c(m,0)[h_l+(-1)^m h_r]. \tag{19}$$

Here h_l and h_r are the surface fields at the $z=0$ and $z=d$ interfaces, respectively. The linear response to these fields is

$$c(z)=\frac{2}{d}\sum_m \cos(\pi mz/d)g(m,0)[h_l+(-1)^m h_r]. \tag{20}$$

The corresponding free energy is

$$F=-\frac{A}{d}\sum_m g(m,0)[h_l+(-1)^m h_r]^2. \tag{21}$$

A. Results for profile and free energy

Using the form Eq. (17) for the structure factor, it is possible to evaluate the linear response profile and free energy of Eqs. (20) and (21) exactly. This calculation is presented in Appendix B, where we obtain the following results:

$$c(z)=(2\xi/q_0)\mathrm{Re}\{ih_l\kappa\cos\kappa(d-z)/\sin\kappa d + ih_r\kappa\cos\kappa z/\sin\kappa d\}, \tag{22}$$

$$F=-(A\xi/q_0)\mathrm{Re}\{i(h_l^2+h_r^2)\kappa\cot\kappa d+2ih_lh_r\kappa\csc\kappa d\}, \tag{23}$$

with κ given by

$$\kappa^2\equiv q_0^2+2iq_0\xi^{-1}. \tag{24}$$

This formula has several properties we expected of the linear-response profile: (1) it evidently has zero integral over the interval $(0,d)$; (2) it is invariant under the interchange of the two interfaces, $h_l\to h_r$ and $z\to d-z$. A typical profile for $d/l=10$ and $q_0\xi=5$ is shown in Fig. 2.

In the limit $\xi\gg q_0^{-1}$, we can further simplify Eq. (22) by approximating

$$\kappa\approx q_0+i\xi^{-1}. \tag{25}$$

Using this approximation, and expanding to leading order in $1/(q_0\xi)$, we obtain for the case of a film of commensurate thickness ($q_0d=n\pi$)

$$c(z)\approx[2\xi/\sinh(d/\xi)]\{h_l\cos[q(d-z)]\cosh[(d-z)/\xi] + h_r\cos(qz)\cosh(z/\xi)\}. \tag{26}$$

In a symmetric film, with $h_l=h_r=h_s$, this yields

$$c(z)=\{2\xi h_s/\sinh[d/(2\xi)]\}\cos[q(z-d/2)]\cosh[(z-d/2)/\xi]. \tag{27}$$

The behavior near a single interface at $z=0$ can be obtained by taking $d\gg\xi,z$ and $h_r=0$ in Eq. (22), which yields

$$c(z)=(2\xi/q_0)h_l\mathrm{Re}\{\kappa e^{i\kappa z}\}\approx 2\xi h_l\cos(q_0z)e^{-z/\xi}. \tag{28}$$

The first line in Eq. (28) is the exact linear-response expression for a single interface, derived previously by Fredrickson, [16] while the second uses approximation Eq. (25) for κ, and shows that this profile is a damped exponential.

Use of the linear-response results makes sense only as long as the induced amplitude $c(z)$ remains small compared to the amplitude a_c of the ordered state at the transition temperature, so that the value of $f_B(\psi)$ can be approximated by a harmonic expansion around the disordered minimum. For the linear response to be valid, the surface field h_s at either boundary must thus satisfy

$$h_s\lesssim h_s^*\equiv a^*/\xi^*=\alpha^{2/3}\lambda^{1/6}=3.226\overline{N}^{-5/6}, \tag{29}$$

where the last relation expresses the scaling of ψ_c and ξ near the transition.

Assuming the linear-response regime can be achieved experimentally, Eq. (22) can be compared directly to experimental concentration profiles obtained from reflectivity [1,2,4]. One simple but important application of this comparison would be to measure the correlation length in a thick film just above the bulk transition temperature, by comparing the experimental profile to Eq. (28). The large but finite value of the correlation length at the transition is a key sig-

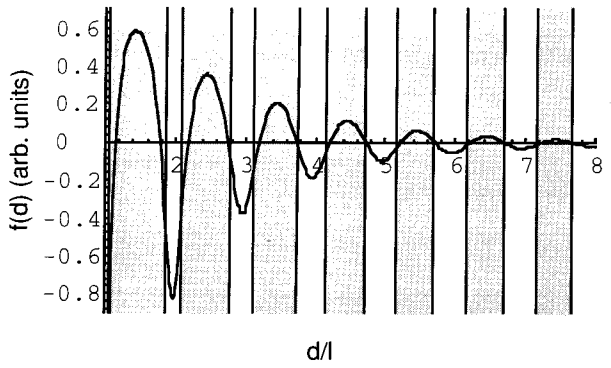

FIG. 3. Linear-response free energy per area as a function of film thickness d, with $q_0\xi=10$. Regions unstable to capillary waves are shaded.

nature of the Brazovskii theory. Reflectivity should afford better resolution in determining the correlation length than bulk small-angle neutron scattering.

Very crudely, a typical surface energy might be on the order of χ per monomeric area on the interface, without special efforts to make the surface neutral with respect to the two blocks of the copolymer. In the vicinity of the order-disorder transition, which is predicted in mean-field thory to occur when $\chi N=10.5$, a typical surface energy might thus be of order $10/N$. This is to be compared to the characteristic surface energy $h_s^* a^* = f^* \xi^* = \alpha = 1.807/N$. This suggests that without special efforts, surface fields at the transition temperature might tend to be in the vicinity of the characteristic field h_s^*. Existing neutron reflectivity experiments seem to be close to this situation; in some cases, the surface fields induce order with an amplitude comparable to that in the bulk ordered state at the transition, [1] whereas in other cases the surface fields induce order of distinctly weaker amplitude [4]. Perhaps with some care in treating surfaces, smaller or larger fields can be achieved, so that both the linear-response and the saturation regime can be observed. Tunable surface fields have been achieved in one copolymer system with surface layers of random copolymers of controlled composition [2].

We now turn to the linear-response free energy, Eq. (23). This expression can be used to identify regions of layer thickness d that would be unstable to capillary waves, using the criterion $\partial^2 F/\partial d^2 < 0$. A plot of this linear-response free energy for a symmetric film (with $h_l = h_r$) as a function of d/l ($l = 2\pi/q_0$), for $q_0\xi = 10$, is shown in Fig. 3.

An important limit is the strongly correlated film ($d \ll \xi$), for which it is simplest to begin again with Eqs. (20) and (21) for the concentration field and free energy. In the limit $d \ll \xi$, the sums over modes are dominated by the term with k_m closest to q_0, i.e., for $m = \mathcal{R}(d/l)$, for which $g(m,0)$ is largest. [The operation $\mathcal{R}(x)$ denotes the nearest integer to x.] Here we are assuming an even number of layers, in response to fields of the same sign on both surfaces. The corresponding k_m is given by $k_m = q_0 + \delta q(d)$, where

$$\delta q(d) = q_0 \left[\frac{\mathcal{R}(d/l)}{d/l} - 1 \right]. \tag{30}$$

This sawtooth variation in the wave number (or equivalently the layer spacing) as the layer thickness is varied has been observed in reflectivity experiments and discussed previously [2].

The corresponding expressions for the concentration field and the free energy in this strongly correlated limit are

$$c(z) \approx \frac{2}{d}(h_l + h_r) \frac{\cos\{[q_0 + \delta q(d)]z\}}{r + [\delta q(d)]^2}, \tag{31}$$

$$F \approx -\frac{A}{d} \frac{(h_l + h_r)^2}{r + [\delta q(d)]^2}. \tag{32}$$

B. Capillary-wave instabilities

The variation of the linear-response free energy with film thickness can induce instabilities to capillary waves even at temperatures above the transition temperature. This phenomenon has previously been considered theoretically by Shull in numerical mean-field calculations [17]. As discussed in the Introduction, the instability is analogous to spinodal decomposition in the bulk; ordered films of even slightly incommensurate uniform thickness can be thermodynamically unstable towards the formation of a two-dimensionally ''phase separated'' state in which one ''island'' or ''hole'' takes up the excess or missing material. The formation of such islands and holes may either be nucleated or grow spontaneously from capillary waves. The coarsening of these islands and holes has been extensively studied experimentally, [18,19] but the early stages of island-hole formation have received less attention.

The instability condition for the growth of capillary waves on the surface of the film is that the free energy per unit area as a function of film thickness be ''concave downwards,'' $\partial^2 \Delta F/\partial d^2 < 0$. Figure 3 shows $\Delta F(d)$ of Eq. (23), together with the regions of instability, for a value of $q_0\xi = 10$.

Note that the regions of stability are independent of the strength of the surface field, which may at first sight seem a strange result. Consider the stabilizing effects of gravity and surface tension. The free energy per unit area of a capillary wave $h(x) = 2h_q \cos(qx)$ becomes

$$F_{\text{cap}} = [F''(d)/A + \rho g + \gamma q^2] h_q^2. \tag{33}$$

Hence, when $F''(d)/A + \rho g < 0$, spinodal instabilities will occur for wave numbers satisfying

$$q^2 < [F''(d)/A + \rho g]/\gamma. \tag{34}$$

We now estimate the relative magnitudes of the curvature $F''(d)/A$ of the free energy and the gravitational term ρg. In the strongly correlated limit, the scale of $F''(d)/A$ from Eqs. (30) and (32) turns out to be $F''(d)/A \sim (h_s^2 \xi^2/d)(d/l)^2 (1/\xi^2)$. Note that the free energy per area itself from Eq. (32) scales as $F(d)/A \sim (h_s^2 \xi^2/d)$. At the characteristic values $h_s = h_s^*$ and $\xi = \xi^*$, the free energy per area is of order $F(d)/A \approx f^* \xi^* (\xi^*/d) = 1.805/N(\xi^*/d)$. To return to physical units (cgs), we multiply by $k_B T/{l_p}^2 \approx 5 \times 10^{-14}/(2 \times 10^{-8})^2 = 125$.

Assuming typical values for a relatively thin, strongly ordered film of $d/l = 5$, $\xi/d = 5$, $N = 10^3$, and $l = 300$ Å, we

find $F(d)/A \sim 1$ erg/cm^2 and $F''(d)/A \simeq (25$ erg/cm$^2)/\xi^2 \simeq 5\times 10^9$ erg/cm^4. This is much larger than $\rho g \simeq 10^3$ erg/cm^4, so the effects of gravity can be completely ignored. Using the same values for d/l, ξ/d, and N and a typical value of $\gamma \simeq 10$ erg/cm^2 for the surface tension, we obtain a critical value of $q_c^2 = F''(d)/(A\gamma) \simeq 2.5/\xi^2$. Hence the upper cutoff to unstable capillary waves, for surface fields of the order of the characteristic field h_s^* is of order the inverse characteristic correlation length $1/\xi^*$.

Experimentally, there are no reports to date of capillary-wave instabilities in advance of the ordering transition in the film. Simultaneous specular reflectivity and grazing incidence diffraction measurements would be required to look for film ordering (or lack of it) and surface roughening due to capillary waves. There is general indirect evidence for a spinodal route to the formation of islands and holes on the surface of copolymer thin films, in that films near a half-integer number of layers have been reported to take much less time to exhibit islands and holes than is required for films near an integer number of layers (for which island and hole formation is presumably nucleated) [20].

IV. GRADIENT EXPANSION

The behavior of thin films of diblock copolymer lamellar phases is one of a class of problems in which spatial inhomogeneity is present, either because of the geometry or because of imposed spatially varying fields such as surface fields. In these problems, we expect the amplitude of microphase separation to vary in space, with distance from the surfaces or other localized disturbances.

If the degree of microphase ordering varies slowly in space, we expect that the free energy is well represented by a gradient expansion, in which we represent the microphase separation in terms of its amplitude $\psi(r)$ and phase $\phi(r)$:

$$c(r) = \psi(r)[e^{iq_0 z + i\phi(r)} + \text{c.c.}]. \tag{35}$$

The fast spatial variation of $c(r)$ on the scale q_0^{-1} is contained in the oscillating phase factor $\exp(i\vec{q}_0 \cdot \vec{r})$; $\psi(r)$ and $\phi(r)$, respectively, represent slow variations in the amplitude or phase of the microphase separation $c(r)$.

The free energy functional $F[\psi(r), \phi(r)]$ then takes the form

$$\begin{aligned} F[\psi(r),\phi(r)] = \int dr \Bigg\{ & f_B(\psi) + \mu_z(\psi)\left(\frac{\partial \psi}{\partial z}\right)^2 + \mu_\perp(\psi) \\ & \times (\nabla_\perp \psi)^2 + B(\psi)\left(\frac{\partial \phi}{\partial z}\right)^2 + \kappa(\psi)(\nabla_\perp{}^2 \phi)^2 \\ & + \cdots - [h_l \delta(z) + h_r \delta(z-d)] \\ & \times 2\psi \cos(q_0 z + \phi) \Bigg\}. \end{aligned} \tag{36}$$

Here $f_B(\psi)$ is the Brazovskii free energy of a uniformly ordered state of amplitude ψ, i.e., the solution from Eqs. (7). The final term represents the surface fields h_l and h_r on the two interfaces.

The coefficients $\mu(\psi)$, $B(\psi)$, and $\kappa(\psi)$ can be calculated systematically from the Brazovskii Hamiltonian Eq. (3). The coefficients $B(\psi)$ and $\kappa(\psi)$ are the smectic compressional and bending moduli (taken at fixed amplitude ψ). They arise from substituting the form Eq. (35) into the Brazovskii free energy $f_B(a)$ and expanding the gradient terms; the absence of a term $(\nabla_\perp \phi)^2$ is dictated by rotational invariance [22]. We are concerned in this paper only with variations along the layering direction $\hat{z}$, so $\mu_\perp$ and κ are not of interest.

It is easy to show, by considering the Brazovskii free energy for a state that is ordered at a wave number q differing slightly from q_0, that $B(\psi) = \psi^2$ exactly. The calculation of the coefficient $\mu_z(\psi)$ is more involved, and is presented in Appendix A by carrying out a gradient expansion of the Brazovskii (or Hartree) free energy of an inhomogeneous system. The essential result is that $\mu_z(\psi)$ varies by only 20% as ψ ranges from zero to a_c, the amplitude at the bulk first-order transition, and that $\mu_z(0) = 1$. Having taken pains to compute $\mu_z(\psi)$ carefully, for simplicity we approximate $\mu_z(\psi) \simeq \mu_z(0) = 1$ in what follows. With this approximation for μ_z, the free energy per unit area for a thin film can be written with surface field terms as

$$\begin{aligned} F/A = \int dz \left\{ f_B(|\Psi|) + \left| \frac{d\Psi(z)}{dz} \right|^2 \right\} - 2\,\text{Re}\{ & h_l \psi(0) \\ & + h_r \psi(d) e^{iq_0 d}\}, \end{aligned} \tag{37}$$

where $\Psi(z) \equiv \psi(z) e^{i\phi(z)}$ is a single complex order parameter.

The gradient expansion is well controlled, for the variations of ψ at least, for sufficiently weakly first-order transitions. The usual argument applies: successive terms in the gradient expansion are multiplied by additional powers of some length, which should be of the order of $l \sim q_0^{-1}$. Then, since the transition is weakly first order, the first two terms in the gradient expansion, of form $(r + q^2)\psi(q)\psi(-q)$, determine a correlation length $\xi = r^{-1/2}$, which is large compared to l. Then as ψ varies on the scale ξ, higher-order terms in the gradient expansion will be smaller by powers of $1/(q_0 \xi) \ll 1$.

Recall that the application of the self-consistent Hartree approximation to the Brazovskii Hamiltonian Eq. (3) is only justified when the transition is nearly second order, for which the correlation length at the transition ξ_c is large compared to the microphase period, or $q_0 \xi_c \gg 1$. Consequently, the use of a gradient expansion will be valid in almost all cases where the use of Brazovskii's approximation for the free energy is itself valid. For the self-consistent Hartree approximation to apply to a film of thickness d, we must have one of the following cases: (1) $1/q_0 \ll \xi \ll d$, so the film is many layers thick and the two surfaces of the film do not communicate, and we have essentially a semi-infinite slab. (2) $1/q_0 \ll \xi \approx d$, so the order extends across the middle of the film, but is not uniform, and the film remains many layers thick. (3) $1/q_0 \lesssim d \ll \xi$, in which case the film may be only a few layers thick but the entire film is strongly correlated and so the amplitude $\psi(r)$ must be spatially uniform. If we consider the case of a film with $\xi \lesssim 1/q_0$, such a correlation length is too short for the self-consistent Hartree approximation to apply. In the limit of very long polymers, however, such short correlation lengths occur only at temperatures well above the ordering transition, at temperatures for which

the effects of fluctuations become small. However, since the self-consistent Hartree approximation reduces to Leibler's mean-field approximation in the limit of high temperatures, this case can often be treated as well.

Note that the variables $\psi(z)$ and $\phi(z)$ must satisfy a constraint,

$$\int dz c(z) = 0, \tag{38}$$

on the average composition of the film, which must vanish because we consider symmetric copolymers for which there can be no excess of A or B monomers. This constraint must be added explicitly because the gradient expansion of the free energy (unlike the linear response approximation of Sec. III) does not by itself contain enough information about chain stretching energies to rigorously exclude states that do not satisfy this constraint. We note, however, that when $\psi(z)$ and $\phi(z)$ are very slowly varying functions (as is assumed in the use of a gradient expansion) then the contributions to Eq. (38) from regions far from the walls of the film will automatically be small due to the rapid oscillation of $c(z)$ and the resulting cancellation of regions of positive and negative c. The most important contributions to Eq. (38) arise instead from regions within a half-period of either boundary, where this cancellation is destroyed by the presence of a sharp wall. In the limit $q_0 \gg \xi^{-1}$ in which $\psi(z)$ and $\phi(z)$ remain nearly constant over distances of order $1/q_0$, the constraint can be satisfied only by taking the values of the phase angle

$$\theta(z) \equiv q_0 z + \phi(z) \tag{39}$$

at each boundary to be very close to some integer multiple of π.

This observation can be made more precise by repeatedly integrating Eq. (38) by parts to generate a power series

$$0 = \mathrm{Re}\left[\frac{e^{iq_0 z}}{iq_0} \Psi(z) + \frac{e^{iq_0 z}}{{q_0}^2} \Psi'(z) + \cdots \right] \Bigg|_{\substack{z=0 \\ z=d}} \tag{40}$$

for the integral in powers of $1/q_0$, or, more precisely, in powers of the operator $q_0^{-1} d/dz$ acting on the complex variable $\Psi(z)$.

To lowest order in $1/q_0$ Eq. (40) is satisfied by taking $\sin(\theta) = 0$ at both boundaries. At the next order in $1/q_0$, Eq. (40) yields boundary conditions at $z = 0$ and $z = d$:

$$0 = \mathrm{Re}\{\Psi'(0) - iq_0 \Psi(0)\},$$
$$0 = \mathrm{Re}\{[\Psi'(d) - iq_0 \Psi(d)] e^{iq_0 d}\}. \tag{41}$$

Here we have assumed that the contributions from each boundary must vanish independently, since it is unphysical in a system of copolymers to satisfy the integral constraint by transferring excess A or B monomers from one side of the film to the other.

Within the context of a gradient expansion for F, it is sufficient to replace the full constraint Eq. (38) by the first few terms in the expansion Eq. (40), which constrains only the surface values and derivatives of $\psi(z)$ and $\phi(z)$. We introduce the constraints of Eq. (41) into the free energy Eq. (37) by means of Lagrange multipliers λ_l and λ_r multiplying the right-hand sides of Eq. (41) and subtracting from F/A.

We then minimize the free energy with an added constraint term with respect to Ψ (we vary with respect to Ψ^*, and take Ψ and Ψ^* to be independent variables), generating Euler-Lagrange equations

$$0 = \Psi \frac{df_B(|\Psi|)}{d|\Psi|^2} - \frac{d^2\Psi}{dz^2}. \tag{42}$$

In terms of ψ and ϕ these Euler-Lagrange equations take the form

$$0 = \frac{df_B}{d\psi} + 2\psi \left(\frac{d\phi}{dz} \right)^2 - 2\frac{d^2\psi}{dz^2}, \tag{43}$$

$$0 = \frac{d}{dz} \left(\psi^2 \frac{d\phi}{dz} \right). \tag{44}$$

The boundary conditions arise from varying the surface field and Lagrange-multiplier terms, and from the boundary term in the variation of $|d\Psi/dz|^2$, taking the form

$$0 = \Psi'(d) e^{-iq_0 d} - (h_r + i\lambda_r), \quad 0 = \Psi'(0) + (h_l - i\lambda_l). \tag{45}$$

The imaginary parts of these equations merely determine the values of λ_l and λ_r; the real parts give a physical boundary condition

$$\mathrm{Re}[\Psi'(d) e^{iq_0 d}] = h_r, \quad \mathrm{Re}[\Psi'(0)] = -h_l. \tag{46}$$

From Eqs. (46) and (41) we can derive the boundary condition on the concentration $c(z) = 2\mathrm{Re}(\Psi e^{iq_0 z})$ itself, which is

$$c'(d) = 4h_r, \quad c'(0) = -4h_l, \tag{47}$$

which is the same as the result derived from the exact linear-response solution of Eq. (22).

For simplicity, we will herafter focus on the case of a symmetric film, with equal surface fields $h_l = h_r = h_s$ on either boundary. Cases in which the film has different, and possibly competitive, surface fields are expected to produce a somewhat richer set of phenomena, some of which have been discussed previously in the context of confined binary-fluid mixtures in Ref. [21].

The coupled differential equations (43) and (44) cannot in general be solved analytically. The phase $\phi(z)$ can be expressed in terms of $\psi(z)$ by solving the linear differential equation (44), to obtain

$$\phi(z) = c \int_{d/2}^{z} \frac{dz'}{\psi^2(z')} + \phi(d/2), \tag{48}$$

where c is an integration constant chosen to satisfy the boundary conditions on ψ and ϕ. [We have integrated from $d/2$ to z because in symmetric films we have $\phi(d/2) = 0$.]

Qualitatively, the phase variation is required to give zero concentration integral, and varies most rapidly where phase variation is cheapest, namely, where $\psi(z)$ is small. If $\psi(z)$ vanishes or nearly vanishes somewhere in the middle of the film (as can occur when $\tau > \tau_c$ and $d \gg \xi$), then essentially all of the phase variation happens there, with the result that the

phase shift is nearly constant within each half of the film, and changes rapidly in the middle. This is the limit of two noninteracting wetting layers. If on the other hand the film is strongly correlated so that $\psi(z)$ is nearly uniform across the film (as will occur if $\xi \gg d$) then $\phi(z)$ will vary essentially linearly with z.

The magnitude of the total change in $\phi(z)$ from one side of the film to the other depends strongly upon whether the film thickness is commensurate or incommensurate with the preferred lamellar spacing $2\pi/q_0$. If the film is commensurate, then $\phi(z)$ is forced to be nonzero only by the effects of constraint Eq. (38), which by itself yields small boundary values for $\phi(z)$, as given by Eq. (41), of order $1/(q_0\xi)$. If the film is incommensurate, however, then in order to obtain values of $\theta(z)$ that are nearly integer multiples of π at the boundaries, we must have $\phi(0) \simeq 0$ and $\phi(d) \simeq z\,\delta q(d)$ [where $\delta q(d)$ is defined in Eq. (30)], thus yielding a total phase shift of order unity.

In the next two subsections, we consider two cases in which relatively simple approximations for the profile and free energy can be obtained analytically. In subsection A, we discuss the behavior of weakly ordered films, and recover the basic results of the linear-response theory of Sec. III. In subsection B, we discuss the case of a strongly correlated ($\xi \gg d$) incommensurate film.

A. Linear response revisited

The simplest applications of the gradient expansion occur for weak surface fields h_s, in which the effect of h_s can be computed perturbatively. In the case of a commensurate film, we take advantage of the expected smallness of the phase variable $\phi(z)$ by first solving for $\psi(z)$ in an approximation in which we ignore the effects of a nonzero $\phi(z)$, and then consider the perturbative effects of the phase variation afterward. Within linear response, the order induced by surface fields at temperatures above T_c in a film of thickness d $(0<z<d)$, are then described by the solution of

$$0 = -\partial^2\psi/\partial z^2 + r\psi - h_s[\delta(z) + \delta(z-d)]. \tag{49}$$

(Here $\hat{z}$ is the direction normal to the film, and we have taken for simplicity equal left and right surface fields, $h_l = h_r = h_s$.)

The surface-field terms establish the boundary condition on $\psi(z)$ (to see this, integrate Eq. (49) over a small interval containing the surface) as

$$\partial\psi/\partial z\big|_{z=0} = -h_s, \quad \partial\psi/\partial z\big|_{z=d} = h_s. \tag{50}$$

The solution to Eqs. (49) and (50) is simply

$$\psi(z) = h_s\xi \frac{\cosh[(z-d/2)/\xi]}{\sinh(d/2\xi)}. \tag{51}$$

This solution corresponds to the approximate linear-response result Eq. (27) of Sec. III (where phase effects were also neglected, since a commensurate film with $q_0\xi \gg 1$ was assumed). In the limit that the film is very thick, the amplitude reduces to a decaying exponential at each surface, $\psi(z) \approx h_s\xi\exp(-z/\xi)$.

We now consider the effect on these results of the terms in Eqs. (43)–(44) involving the phase gradients. Combining boundary condition Eqs. (41) and (48) yields

$$\phi(z) = \frac{2\psi'(0)}{q_0\psi(0)} \frac{\int_{d/2}^{z} dz'/[\psi(z')]^2}{\int_0^d dz'/[\psi(z')]^2}. \tag{52}$$

In practice, the effects on the concentration profile of phase shifts for commensurate films are always quite small, and probably not observable. Figure 2 shows the exact linear-response profile for a four-layer film with $q\xi = 5$, compared to the linear-response profile before phase correction, Eq. (51). As is evident from the figure, this is a very short correlation length, for which the gradient expansion in $1/q$ and the zero-integral constraint on the uncorrected profile might be expected to be in error. The first phase correction, using the phase from Eq. (52) (integrated numerically), is shown as the dashed line. Even for this case, the phase variation is less than 0.2 rad. The concentration profile computed using the amplitude variation Eq. (51) and the phase correction Eq. (52) would be indistinguishable from the exact profile in this figure.

If the film is incommensurate, there is a competition between the constraints imposed upon the boundary values of the phase by the integral constraint and the surface fields, and the cost of distorting the wave number in the ordered portions of the film. If ξ and d are of comparable magnitude, this leads even in the linear response regime to coupled equations for $\psi(d)$ and $\phi(d)$ that cannot be solved analytically. If $\xi \ll d$, so that ordered regions near both boundaries are separated by a region of nearly vanishing ψ, than this frustration can be relieved by allowing ϕ to take a rapid jump between its boundary values of $\phi(0) \simeq 0$ and $\phi(d) \simeq d\,\delta q(d)$ over a region of width ξ in the middle of the film. If $\xi \gg d$, so that $\psi(z)$ is nearly constant across the film, we instead expect a linear variation

$$\phi(z) = z\,\delta q(d) = z q_0 \left[\frac{\mathcal{R}(d/l)}{d/l} - 1\right] \tag{53}$$

of the phase to ''stretch'' or ''compress'' the wave number to a commensurate value. This is precisely the behavior found experimentally in Ref. [2], and reproduced in Sec. III in the strongly correlated limit, Eq. (32).

From Eq. (36), we see that such a phase variation imposes an additional cost $\psi^2[\delta q(d)]^2$ in the free energy density, which amounts to replacing the inverse susceptibility r by $r + [\delta q(d)]^2$. So the induced spatially uniform amplitude and linear-response free energy in this case become

$$\psi = h_s/\{r + [\delta q(d)]^2\}^{1/2},$$

$$\Delta F = -2h_s^2/\{r + [\delta q(d)]^2\}^{1/2}, \tag{54}$$

which are precisely the results of Eq. (32).

B. T_c shifts ($\xi \gg d$)

The simplest case in which to consider the effects of commensurability beyond linear response, as is required to address shifts in the first-order transition temperature, is a strongly correlated film in which $\xi \gg d$. Then it is clear that

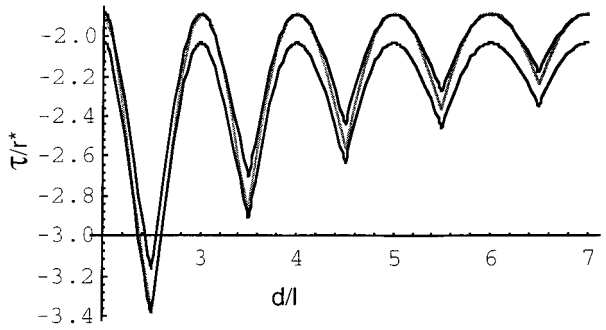

FIG. 4. In strongly correlated incommensurate films ($\xi \gg d$) with no surface field, the phase $\phi(z)$ varies linearly to enforce the zero-integral constraint. The result is that $\tau_c(d)$ and $\tau_s(d)$ (upper and lower dark curves, plotted in dimensionless units defined in Sec. II B) are oscillating functions of d. Above the shaded curve, the ordered state where it exists is unstable to capillary waves. Here $q_0\xi = 5$.

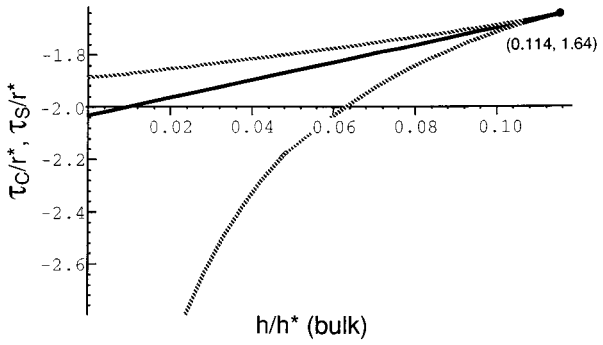

FIG. 5. The phase behavior of the Brazovskii model in the presence of a nonzero field conjugates to the amplitude a, in the dimensionless units defined in Sec. II B. The line of first-order transitions (solid) and the corresponding spinodals (metastability limits of the ordered and disordered phases) (dotted) meet at a critical point, $h = 0.114h^*$, $\tau = -1.64r^*$.

the amplitude $\psi(z)$ is independent of z, and the phase $\phi(z)$ varies linearly as given by Eq. (53).

In the absence of surface fields, the free energy per unit volume of Eq. (37) then becomes

$$f = f_B(\psi) + \psi^2[\delta q(d)]^2. \tag{55}$$

The stretching of the phase to give commensurability and thus zero concentration integral gives a d-dependent quadratic shift in the free energy density. Recall that $f_B(\psi)$ is very well represented by the sixth-order polynomial $f_p(\psi)$ of Eq. (13). If only the quadratic coefficient c_1 of f_p varied significantly with temperature near the transition (which is the natural simplification for second-order transitions, since there the quadratic coefficient vanishes), then the commensurability effects would amount to a shift in $T - T_c$. However, at a first-order transition, none of the coefficients $\{c_i\}$ is vanishing, and so we cannot argue that the temperature variation of the quadratic term is dominant.

Instead, we simply replace $f_B(\psi)$ with $f_p(\psi)$ in Eq. (55), and compute the resulting spinodal and transition temperatures as a function of d. The size of the commensurability-induced shifts in τ_c and τ_s depends on the near divergence in the correlation length, which can be characterized by $q_0\xi^*$ as discussed in Sec. II B. The results are shown in Fig. 4, for $q_0\xi^* = 5$. Note that the effects of commensurability are most pronounced for the thinnest films, as one would expect; it is progressively easier for the phase to adjust the film thickness by at most half a layer, as the film is made thicker. Note that the variations in the transition and spinodal temperatures as a function of film thickness can be quite large on the scale of the difference $\tau_s - \tau_c$. In other words, if an experiment can resolve the difference between the bulk spinodal and transition temperatures, it has sufficient temperature resolution to see the commensurability-induced shifts in the transition temperature.

These commensurability effects also give rise to capillary-wave instabilities of the ordered phase, since its free energy per unit area becomes an oscillating function of the film thickness. The film free energy per area as a function of d can be shown to be concave down and hence unstable in regions of d near half-integer layer thickness. We have implicitly assumed here that there is some surface field acting that selects one of the two blocks at the surface. If the surface field were strictly zero, either block could appear at either surface, and the film would be commensurate if it were a half-integer number of layers thick. Then Eq. (53) would be replaced by a similar expression with l replaced by $l/2$.

The width of the unstable regions depends on the temperature, and can be defined for any temperature below the spinodal temperature t_s at which a second minimum in the free energy first appears. In the region in the t-d plane above the shaded curve in Fig. 4, the (metastable) ordered state is unstable to capillary waves.

Note that within the gradient-expansion picture, there is no spinodal instability of the *disordered* phase with $h_s = 0$, since the free energy is just that of the bulk disordered phase independent of d. This misses some interesting physics, however, which can be recovered in a self-consistent Hartree approximation applied directly to a film of finite thickness: capillary-wave instabilities can result from commensurability effects on the fluctuation spectrum and hence the free energy of the disordered phase even with $h_s = 0$ [23].

The effects of commensurability remain qualitatively similar in the presence of a moderate surface field. The free energy per unit volume of a strongly correlated film with surface fields $h_s = h_l = h_r$ can be written as

$$f = f_B(\psi) + \psi^2[\delta q(d)]^2 - 4\psi h_s/d, \tag{56}$$

where the last term represents the contribution of the surface field. This is the free energy of a Brazovskii model with a shifted quadratic coefficient in the presence of an effective bulk field

$$h_{\text{eff}} = 2h_s/d \tag{57}$$

conjugate to the uniform amplitude $\psi = a$.

In a commensurate film, with $\delta q(d) = 0$, the effect of such an *effective* bulk symmetry breaking field is to produce a nonzero value for ψ in the disordered state and to decrease the value of ψ in the ordered state just below the transition temperature, thus decreasing the discontinuity in ψ at the transition, and also to raise somewhat the transition temperature.

For strong enough $h_{\rm eff}$, the discontinuity disappears completely, thus causing the line of first-order transitions in the $(h_{\rm eff}$-$\tau)$ plane to end at a critical point

$$h_{\rm crit}=0.114h^*, \quad \tau_{\rm crit}=-1.64r^* \tag{58}$$

with $h_{\rm eff}=h_{\rm crit}$ of order the characteristic value effective bulk field $h^*\equiv a^*/\xi^{*2}$. The corresponding phase behavior for a commensurate field with a free energy density of form (56) is shown in Fig. 5, where the first-order transition is shown as a solid line and the corresponding spinodals (limits of metastability of the ordered and disordered phases) are shown as dotted lines. The existence of a critical point implies that the presence of a sufficiently large surface field, large enough so that $h_{\rm eff}(d)>h_{\rm crit}$, will destroy the discontinuous transition, leading instead to a smooth evolution of the degree of order with decreasing temperature.

For $0<|h_{\rm eff}|<h_{\rm crit}$, the transition temperature $\tau_c(h)$ varies almost exactly linearly with $h_{\rm eff}$ from $\tau_c(h_{\rm eff}=0)=-2.03r^*$ to $\tau_c(h_{\rm crit})\equiv\tau_{\rm crit}$. This nearly linear variation of τ_c with the strength of the effective bulk field, together with the $1/d$ dependence of $h_{\rm eff}$ upon d suggests that the transition temperature for strongly correlated commensurate films with different numbers of layers should vary as

$$\tau_c(d)-\tau_c^{\rm bulk}\propto h_s/d \tag{59}$$

for $h_{\rm eff}<h_{\rm crit}$.

The d dependence of the critical temperature in a set of films with a fixed surface field, with h_s small enough so that $h_{\rm eff}<h_{\rm crit}$ for the thicknesses of interest, is given by a combination of the two effects described above. The transition temperature oscillates with d in a manner similar to that predicted for $h_s=0$, but the maxima of τ_c at commensurate values of d are always somewhat higher than the bulk transition temperature and less than $\tau_{\rm crit}$, with a slow variation of τ_c at consecutive maxima given by Eq. (59).

V. WETTING ANALOGIES

We return now to films of commensurate thickness, but with surface fields h_s that may be strong enough so that linear response calculations are inadequate. Because of the discussion and examples of Sec. IV, we neglect the phase variable. Then we recover a variation on a classical problem, that of wetting phenomena in a finite slab between two surfaces of a mixture of liquids near the demixing critical point. The amplitude $\psi(z)$ plays the role of the concentration variable in the two-fluid problem. The free energy density Eq. (36) is of precisely the form considered by Cahn in his seminal works on prewetting phenomena near the liquid-liquid critical point, [24,25] a square-gradient term plus a free energy function with two competing minima.

There are several important differences between the case of copolymer thin films and the systems considered in Refs. [24,25]. Our order parameter [the amplitude $\psi(z)$] is not conserved, which has two immediate consequences. First, there can be coexistence between ordered and disordered copolymer phases only at a temperature exactly equal to the transition temperature, making coexistence unlikely to be observed in practice. (In the case of a two-fluid mixture, two phases can coexist with different amounts of fluid A, and the corresponding chemical potential equal in the two phases, allowing coexistence to occur over a nonzero range of temperatures, and to thus be easily observed.) Second, the dynamical behavior of our nonconserved order parameter is qualitatively different from that of a conserved order parameter: Material does not have to be transported large distances to relax a slowly varying amplitude profile, as it does for a conserved order parameter. Finally, our free energy density is of a different form from the canonical $t\psi^2+a\psi^3+b\psi^4$ considered in Ref. [24], which leads to differences in the shape of interfacial profiles.

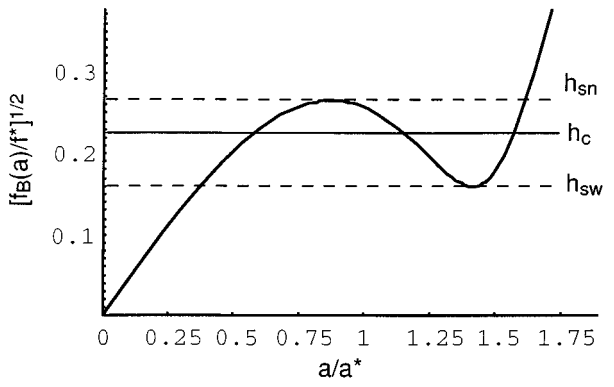

FIG. 6. A plot of the Cahn construction, $[f_B(\psi)]^{1/2}$ vs ψ, in dimensionless units, for a reduced temperature $\tau_c<\tau=-2.0r^*<\tau_s$, with values of h_s (horizontal lines) corresponding to the spinodals h_{sw} and h_{sn} of the wet and nonwet states, and to the prewetting transition field h_c.

A. A single interface

We now review briefly Cahn's results for a binary fluid mixture with a single boundary at which a surface field is applied. The free energy per unit area is that of Eq. (36) without the phase terms,

$$F=\int_0^\infty dz[f_B(\psi(z))+[\psi'(z)]^2-2h_s\delta(z)\psi(z)]. \tag{60}$$

By measuring distances in units of ξ^*, concentration amplitude ψ in units of a^*, free energy density in units of f^*, and surface field in units of h_s^* we can reduce Eq. (60) to a ''universal'' form. Thus we can give a universal prewetting phase diagram, as a function of reduced temperature τ, normalized surface field strength h_s/h_s^* and film thickness d/ξ^* when we consider films of finite thickness.

The optimum profile minimizes F,

$$0=\frac{\partial f_B}{\partial\psi}-2\psi''-2h_s\delta(z). \tag{61}$$

Integrating over the δ function gives the boundary condition

$$\psi'(z)|_{z=0}=-h_s. \tag{62}$$

Away from the boundary, Eq. (61) has a first integral,

$$c=[\psi'(z)]^2-f_B(\psi(z)), \tag{63}$$

where c is a constant to be determined.

For a semi-infinite system above the bulk transition temperature, we have $\psi=\psi'=0$ far from the interface, and so $c=0$ in Eq. (63). Then we have

$$\psi'(z)=[f_b(\psi(z))]^{1/2}, \tag{64}$$

which can be used to compute the shape of the profile. This result can also be used to eliminate the need to know the shape of the profile if all we want is to compute the free energy of the interface; using Eq. (64) we have

$$F(\psi(0))=2\int_0^{\psi(0)} d\psi[\sqrt{f_B(\psi(z))}-h_s]. \tag{65}$$

This key result of Ref. [24] leads to a graphical representation of the possible amplitude profiles at the interface and their free energies. Figure 6 shows a typical graph of $\psi'=\sqrt{f_B(\psi)}$ as a function of ψ for some temperature (or effective temperature τ) below the spinodal temperature at which a second metastable minima appears in f_B, and hence in $\sqrt{f_B}$ (i.e., $\tau<\tau_s$), but above the bulk transition temperature (i.e., $\tau>\tau_c$). A horizontal line represents a value of surface field h_s; the intersections with the curve give possible values of $\psi(0)$ for which Eq. (62) is satisfied.

For $h_{sw}<h<h_{sn}$, there are three such intersections, corresponding to three values of $\psi(0)$ and hence to three distinct profiles $\psi(z)$ for which the free energy is stationary under perturbations. The largest value of $\psi(0)$ is slightly larger than that of ordered-phase minima in $f_B(\psi)$, and corresponds to a profile that as the temperatures approaches the bulk transition temperature evolves into one in which there exists a well-defined ''wetting layer'' of bulklike lamellar order near the boundary, in which the value of ψ remains near that in the bulk ordered phase, with a thickness that diverges continuously as the transition temperature is approached from above. The middle intersection can be shown to correspond to a local maximum in the free energy, rather than a local minima, and is thus not a physically relevant state. The smallest value of $\psi(0)$ is similar in magnitude to that which would be predicted by linear-response theory, and corresponds to a profile in which $\psi(z)$ decays to zero within about a bulk correlation length of the boundary even at the transition temperature. We will refer to the two solutions corresponding to local free energy minima (throughout the range of reduced temperatures $\tau_c<\tau<\tau_s$ for which two such solutions exist) as the ''wet'' (i.e., interface is wet by the ordered lamellar phase) and ''nonwet'' (interface is not wet by the ordered phase) states, and to the corresponding values of ψ at the boundary as $\psi_{\rm wet}$ and $\psi_{\rm nonwet}$. Our use of ''wet'' and ''nonwet'' to describe states at temperatures slightly above the transition temperature is adopted for simplicity, but, it should be noted, is a slight generalization of conventional nomenclature for wetting, which holds that a state can be described as ''wet'' only when there exists a macroscopically thick wetting layer, which can occur only exactly at the transition temperature [25].

Twice the integrated area between the curve $\psi'(\psi)$ and the horizontal line, from $\psi=0$ to $\psi=\psi(0)$, is exactly the free energy of Eq. (65). From this, it is easy to confirm that the middle intersection point corresponds to a maximum in $F(\psi(0))$, while the other states correspond to local minima. The value h_c is special in that the free energies of these two states are equal,

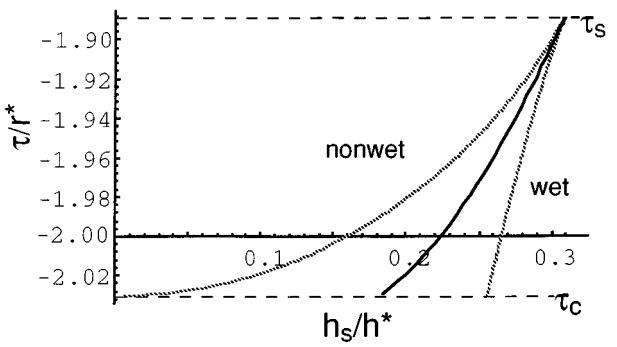

FIG. 7. For a single interface, or an infinite film, the Cahn construction with the Brazovskii free energy gives rise to the prewetting phase diagram shown here, in dimensionless units. The solid line represents the prewetting transition and the dotted lines the spinodals of the two competing surface profiles. The critical point is at $\tau=\tau_s$, $h_s=0.308h_s^*$.

$$F(\psi_{\rm nonwet})=F(\psi_{\rm wet}). \tag{66}$$

Graphically, this corresponds to the zero total area between the line and curve from $\psi_{\rm nonwet}$ to $\psi_{\rm wet}$. Thus $h_c(\tau)$ is a line of first-order phase transitions between the wet and nonwet states; for $h_s>h_c$ ($h_s<h_c$) the wet (nonwet) state is stable.

The surface fields h_{sw} and h_{sn} correspond, respectively, to the limits of metastability (spinodals) for the wet and nonwet states, since for $h>h_{sn}$ ($h<h_{sw}$) the nonwet (wet) state does not exist. As the temperature is increased to the spinodal temperature τ_s, the maximum and minimum in f_B and hence in $\sqrt{f_B}$ merge, as the values of h_c, h_{sn}, and h_{sw} become equal. This is the prewetting critical point.

The values of h_{sn} and h_{sw} can be found explicitly as $\sqrt{f_B(\psi_{sn})}$ and $\sqrt{f_B(\psi_{sw})}$, with $(\psi_{sn})^2$ and $(\psi_{sw})^2$ the solutions of

$$0=f_B'(\psi)=2\psi\{c_1+2c_2\psi^2+3c_3\psi^4\}, \tag{67}$$

where we have approximated the bulk free energy density $f_B(\psi)$ by the polynomial $f_p(\psi)$ given in Eq. (13). The integral $\int d\psi\sqrt{f_p(\psi)}$ can be done analytically, and the value of $h_c(\tau)$ found by solving Eqs. (66) and (62) numerically. The resulting phase diagram is shown in Fig. 7. The critical end point is located at $\tau=\tau_s$, $h_s=0.308h_s^*$.

B. Two interfaces

Sadly, much of this elegant analysis is no longer possible when a film of finite thickness is considered. The reason is that the argument following Eq. (63) that the constant appearing there vanishes, no longer applies, because the amplitude need not vanish at the center of the slab. (This situation has been considered previously by Nakanishi and Fisher, [26] in the context of thin films of binary fluid mixtures.) Since we do not know the value of $\psi(d/2)$ *a priori*, we cannot compute the free energy without knowing a bit more about the profile $\psi(z)$.

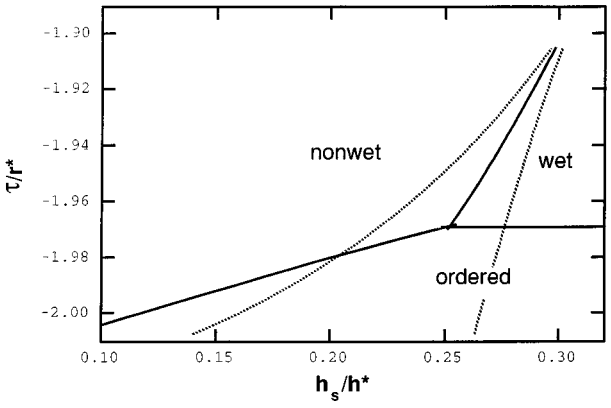

FIG. 8. Wetting phase diagram for a film of finite thickness $d/\xi^*=25$, to be compared to Fig. 7. Note the presence of a ''capillary condensation'' transition between the ordered and wet states at an h-independent temperature higher than that of the bulk ordering temperature, and of the essentially linear surface-field dependence of the ordered to nonwet transition temperature.

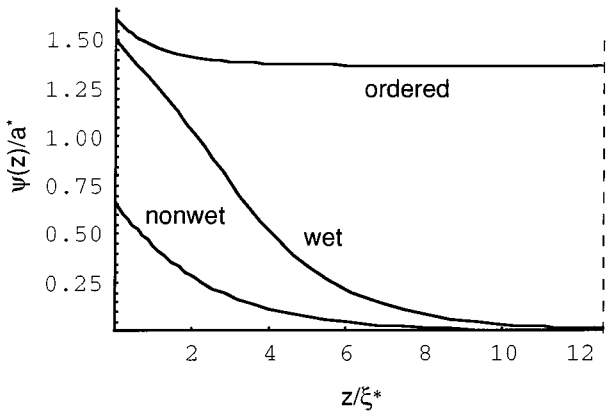

FIG. 9. Typical nonwetting, wetting, and film-ordered profiles (half of full profiles shown, $d/l=20$), for parameter values $\tau=-2.0r^*$ and $h_s=0.225h_s^*$.

The alternative is a more intensively numerical calculation. We replace Eq. (64) with

$$\psi'(z)=\{[f_b(\psi(z))+c]\}^{1/2}, \tag{68}$$

where c is a constant whose value must be determined numerically. In principle, we adjust the values of $\psi(0)$, $\psi(d/2)$, and c for a given τ, h_s, and film thickness d so that the profile $\psi(z)$ has the (1) proper boundary condition at $z=0$ and $z=d$, (2) zero slope in the middle at $z=d/2$, and (3) the proper thickness:

$$\begin{aligned} &\psi'(0)=h_s \quad \text{implies} \quad h_s^2=f_b(\psi(0))+c, \\ &\psi'(d/2)=0 \quad \text{implies} \quad 0=f_b(\psi(d/2))+c, \end{aligned} \tag{69}$$

$$d=2\int_{\psi(d/2)}^{\psi(0)} d\psi/\psi'(z)=2\int_{\psi(d/2)}^{\psi(0)} d\psi/\{[f_b(\psi)+c]\}^{1/2}.$$

Multiple states (wetting, nonwetting, and ordered) and hence multiple values of $\psi(0)$, $\psi(d/2)$, and c are expected for some values of τ, h_s, and d. In practice, to find these states requires sensible initial guesses and a lot of numerical root finding.

The free energy per area for a film of finite thickness then becomes (we have assumed equal surface fields on both surfaces for simplicity)

$$F=4\int_{\psi(d/2)}^{\psi(0)} d\psi\,[f_B(\psi)+c]^{1/2}-cd-4h_s\psi(0), \tag{70}$$

which can be evaluated numerically for the several states once the values of $\psi(0)$, $\psi(d/2)$, and c are known, to determine the location of the various transitions in the phase diagram. The resulting phase diagram is shown in Fig. 8, for a film of thickness $d/\xi^*=25$.

C. Capillary condensation

Apart from direct numerical calculations, we can give some simple arguments that clarify the prewetting behavior of films in the presence of two interfaces separated by a distance d, as the first-order transition is approached from above. Consider the case where d is several times ξ_c, the bulk correlation length at the transition. When the interfaces are nonwet, the induced profiles have a thickness of order ξ, and thus do not interact appreciably across the film. When the prewetting transition line is crossed and the interfaces become wet, their thickness is at first still of order ξ, though perhaps a finite factor larger.

But as $\tau\to\tau_c$, the wet interfaces become thicker. Equation (64) gives some idea of how this occurs, since from it the profile can be computed as

$$\begin{aligned} z(\psi)&=-\int_{\psi(0)}^{\psi} d\psi/\sqrt{f_B(\psi)} \\ &\sim \int d\psi/\sqrt{(\tau-\tau_c)+\text{const}\times(\psi-\psi_c)^2}. \end{aligned} \tag{71}$$

The last crude approximation reflects the fact that as $\tau\to\tau_c$, the free energy of the ordered minimum approaches zero, and so $\partial\psi/\partial z$ very nearly vanishes in the vicinity of ψ_c. Thus the wet profile thus becomes very thick: the small difference $\tau-\tau_c$ cuts off a logarithmic divergence in Eq. (71), so we conclude that the wet layer thickness l grows logarithmically as $l\sim-\xi\ln(\tau-\tau_c)$, and the two wet layers meet in the middle when

$$\tau-\tau_c\sim\exp(-d/\xi). \tag{72}$$

On the other hand, we may compare the free energy of the state consisting of two prewetting layers with a state that is ordered across the entire film, to ask when the thin-film analog of the bulk ordering transition occurs. If we replace the state with two prewetting layers and a disordered middle with a state ordered across the film, we give up two interfaces between ordered and disordered material at the cost of ordering the interior of the film. (See Fig. 9.)

The interfacial tension between the ordered and disordered phases is finite at the transition temperature τ_c, and is of order $\Delta f\xi_c$, where $\Delta f\sim f^*$ is the height of the barrier in the double-well free energy density. The bulk ordering of the middle of the film costs a free energy per area of order

$(\tau-\tau_c)f^*d$, since the region to be ordered is roughly d thick, and the difference between the ordered and disordered state free energy densities scales as $(\tau-\tau_c)f^*$. Equating these two free energies per area, we find that it pays to order the film to get rid of the interfaces at a τ_{wo} given by

$$\tau_{wo}-\tau_c \approx \xi/d. \tag{73}$$

This ordering of the film in advance of the transition is ''capillary condensation,'' since ultimately it derives from the presence of surface fields on the boundaries. For $d>\xi$ the capillary condensation condition Eq. (73) is less stringent than the condition Eq. (72) that the wetting layers begin to overlap.

Note that the strength of the surface fields does not enter the estimate of the shift in τ_c, for the case of wet interfaces. This is because in both the ordered and the wet-interface states, the structures near the boundaries are basically the same, being essentially linear response to the surface field around the ordered state. (See Fig. 9.) Thus the first-order transition between the wet and ordered states should be essentially independent of surface field, which is observed in the numerically computed phase diagram Fig. 8.

Now consider the case where nonwet interfaces make a transition directly to the ordered state. The nonwet interface consists basically of linear response around the disordered state, while the ordered state is essentially the same as the bulk ordered state with a linear-response increase in concentration amplitude at the interfaces. (See Fig. 9.) Thus the free energy per area difference between these two states is approximately $-h_s a_c+(\tau-\tau_c)f^*d$, which leads to a nonwet-ordered transition at a τ of

$$\tau-\tau_c \approx h_s\xi^*/(h_s^* d). \tag{74}$$

Thus the nonwet-ordered transition temperature is shifted upwards from the bulk ordering temperature τ_c by an amount that varies linearly with h_s.

To summarize, we expect for $d \gtrsim \xi$ the structure of the prewetting phase diagram for a thin film should be similar to that of a semi-infinite sample, except that the bulk ordering transition is replaced by a capillary condensation line at a slightly higher temperature, with the nonwet-ordered transition depending linearly on h_s, and the wet-ordered transition approximately independent of h_s. This is consistent with the numerically computed phase diagram of Fig. 8.

VI. DISCUSSION

We have considered a variety of interesting effects that occur when symmetric diblock copolymer melts are confined to a thin film. The thin film has two main influences on the melt. First, surface fields create a layer of the preferred monomer at the surface, which then induces some degree of layering away from the surface, extending at least a bulk correlation length into the film. When the surface fields are sufficiently weak, their effects may be considered in linear response. For this case, the induced concentration profile may be computed exactly (within the Brazovskii theory of the bulk lamellar ordering transition).

Even for thick films, this result provides a useful route to measuring a fundamental quantity characterizing the nearly second-order lamellar transition, namely, the correlation length ξ at the transition. Because this length may be quite long (many lamellar periods, and hence several thousand angstroms), it is difficult to measure using bulk small-angle neutron scattering with the customary resolution limits. A reflectivity experiment is likely to give better resolution for ξ. Such measurements applied to a series of materials of different χ value and hence N value, which according to theory governs the magnitude of first-order behavior, could provide a sensitive test of whether the mean-field limit is approached as $N\to\infty$. There is some indication of puzzling experimental results in this respect: judging from existing reflectivity data, the correlation length from reflectivity in the relatively high-χ system polystyrene-poly(methyl methacrylate) (PS-PMMA) is longer than that in the supposedly more mean-field-like poly(ethylene-propylene)-poly(ethylethylene) (PEP-PEE) system. This correlates with another unexplained feature of the experimental phase diagrams, that the bicontinuous $IA3d$ phase, which is predicted to appear in the mean-field limit, is only observed in systems such as PS-PI (polyisoprene) with *small* values of N, and not in PEP-PEE.

The second effect of the thin-film geometry is what has been termed ''frustration'' in Ref. [2]: the lamellar period is forced to be commensurate with the film thickness. Even in linear response in the disordered phase, there are regions of layer thickness near half-integer values we then predict to be unstable to capillary waves. There is a strong analogy here with spinodal decomposition, in which the thickness of the film plays the role of a conserved variable, and the free energy per unit area must be a convex function of thickness for the film to be stable. The essential physics is that the system can have a stronger response to the surface fields if the damped oscillatory concentration profiles from the two surfaces meet in the middle of the film with the same phase, without adjusting the wavelength of the oscillation away from the preferred value. To test this prediction would require determination of both the state of film ordering (by specular reflectivity) and the surface roughness (by grazing incidence diffraction) under the same conditions.

We have treated copolymer thin films beyond the linear response regime by means of a gradient expansion, justified when the lamellar transition is nearly second order. We write the oscillating concentration profile as a product of a slowly varying amplitude times a cosine with a slowly varying phase. If the phase can be neglected (e.g., for films of commensurate thickness), the resulting effective Hamiltonian is strongly analogous to that used by Cahn in his treatment of wetting and especially prewetting phenomena. In the presence of a single interface, we can have either a ''nonwet'' induced profile, of small amplitude, or a ''wet'' induced profile, of amplitude similar to the eventual bulk-ordered state. There is a line of first-order transitions in the temperature-surface field plane, terminating in a critical end point, precisely analogous to the prewetting line and critical point of Cahn. This prewetting line has been elusive, predicted in 1977 and observed only in 1992 by Taborek and Rutledge [27]. The copolymer system may afford advantages for studying this transition: (1) the order parameter (the amplitude of the concentration wave) is not conserved, so trans-

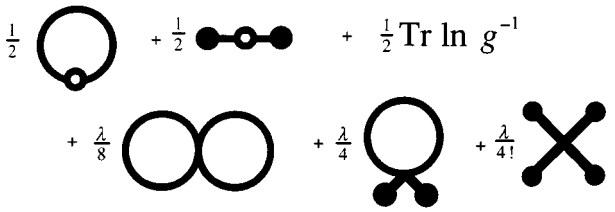

FIG. 10. Diagrammatic expansion for the Brazovskii free energy. Thick lines represent the self-consistent propagator g, open circles represent factors of $g_0^{-1}(q)$, and thick dots represent the expectation value of the concentration field. Signs, combinatorical factors, and factors of the quartic coupling λ are indicated.

port of material is not an issue; (2) the underlying concentration oscillation serves as a ''marker'' to help interpret the reflectivity data; (3) the calculation of the location of the prewetting line in terms of the interaction parameter χ and chain length N is well controlled, does not involve any liquid-state theory, and χ can be extracted from other experiments.

In the thin film geometry, we have the additional possibility of ''capillary condensation,'' previously considered by Nakanishi and Fisher [26] and by Evans *et al.* [9] in the context of binary fluid mixtures. The middle of the film orders above the bulk ordering transition in order to (1) eliminate two interfaces between the ''wet'' state and the disordered middle of the film, if the surface field and temperature are such that the two interfaces are wet; or (2) to take advantage of the increased order at the surface and resulting favorable surface field energy, if the two interfaces are ''nonwet.'' This capillary condensation transition preempts the bulk ordering of the film; we have computed a phase diagram showing the nonwet, wet, and film-ordered phases for a film of typical thickness.

The effects of commensurability beyond linear response can be treated in the case of a strongly correlated film. It is evident that the ''frustration'' of Ref. [2] must give rise to shifts in the ordering transition temperature; as the film is obliged to order at a nonoptimal wave number, the transition temperature is suppressed. We may once again in this situation ask whether or not the film in the ordered state is unstable with respect to capillary waves, and compute regions around the half-integer values of film thickness for which the film would be unstable to capillary waves.

ACKNOWLEDGMENTS

The authors gratefully acknowledge helpful conversations with Frank Bates, Glenn Fredrickson, Anne Mayes, Tom Russell, and Navjot Singh.

APPENDIX A: GRADIENT EXPANSION

Imagine an ordered lamellar phase, with a sinusoidal concentration variation $c_0(\vec{x})=a[\exp(i\vec{q}\cdot\vec{x})+\exp(-i\vec{q}\cdot\vec{x})]$, which is then weakly modulated in amplitude on a much longer wavelength:

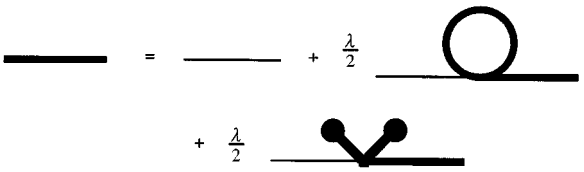

FIG. 11. Diagrammatic equation for the self-consistent propagator g (thick line) in terms of the bare propagator $g_0=[\tau+(q-q_0)^2]^{-1}$ (thin line) and the ordered-state concentration field (thick dot).

$$c(\vec{x})\equiv c_0(x)+\delta c(x)$$
$$=[a+b(e^{i\vec{k}\cdot\vec{x}}+e^{-i\vec{k}\cdot\vec{x}})](e^{i\vec{q}\cdot\vec{x}}+e^{-i\vec{q}\cdot\vec{x}}),$$
$$|k|<<|q|,b\ll a. \tag{A1}$$

The amplitude modulation produces ''sidebands'' in the Fourier representation of $c(\vec{x})$, which are just the new plane waves $\exp[\pm i(\vec{q}\pm\vec{k})\cdot\vec{x}]$. We determine the lowest-order terms in the gradient expansion Eq. (36) by computing the free energy of the modulated concentration profile to $O(b^2)$ and to $O(k^2)$. We do not assume that the amplitude a of the unmodulated pattern is small, so we work to extend the self-consistent Brazovskii calculation to this modulated pattern.

If we simply insert Eq. (75) into Eq. (36), we obtain to the relevant order a free energy density

$$f\approx f_B(a)+\{f_B'(a)+2\mu_z(a)k^2\}b^2+\cdots. \tag{A2}$$

We now perform the corresponding explicit calculation to determine $\mu(a)$. Our starting point is the diagrammatic expression for the Brazovskii free energy of an arbitrary ordered state, Fig. 10, with the corresponding self-consistent equation for the propagator g, represented diagrammatically in Fig. 11 [11,14]. [The thin and thick lines represent the bare and self-consistent propagators g_0 and g, the open circles represent factors of $g_0^{-1}(q)$, and the thick dots represent the ordered concentration field.] Note that for nonperiodic concentration fields, the propagator g is not diagonal in Fourier space.

A systematic expansion of these diagrams to $O(b^2)$ gives for the change in the free energy the diagrammatic expression of Fig. 12, in which the legs ending in a ''T'' represent factors of the perturbation δc to the concentration field. (The set of diagrams of Fig. 12 could almost have been written

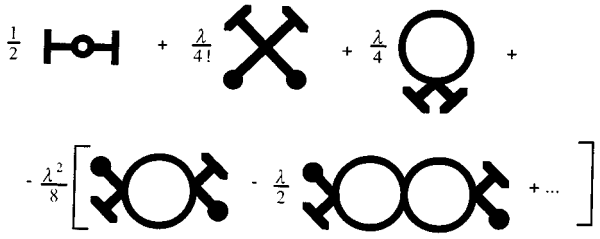

FIG. 12. Diagrammatic expansion of the Brazovskii free energy to second order in the perturbation $\delta c(z)$ of the concentration field away from that in a bulk equilibrium state. Diagrammar as in Figs. 10 and 11, with legs ending in a ''T'' representing factors of δc.

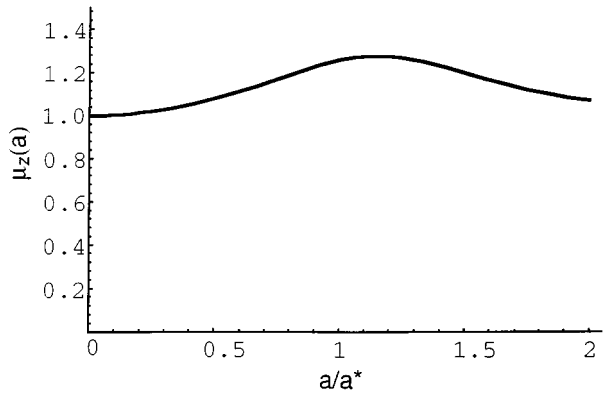

FIG. 13. The square-gradient coefficient $\mu_z(a)$ depends only mildly on the ordered-state amplitude a over the relevant range of a (curve shown for the transition temperature of $\tau=-2.031r^*$, at which the ordered-state amplitude is $a=1.455a^*$).

down as a starting point, as the obvious set of connected diagrams with no external lines, second order in δc, using the quartic vertex of the Brazovskii Hamiltonian and the self-consistent propagator.)

The series of bubble diagrams represented by the first two terms in brackets can be summed in terms of the single-bubble integral, given by

$$\Pi(\vec{k})\equiv\int\frac{d^3q}{(2\pi)^3}[r+(q-q_0)^2]^{-1}[r+(p-q_0)^2]^{-1},\qquad \vec{p}\equiv\vec{q}+\vec{k}. \tag{A3}$$

In terms of the bubble-sum $\chi(\vec{k})\equiv[1+\lambda\Pi(\vec{k})/2]^{-1}$, the diagrams of Fig. 12 give

$$\delta f=2\left\{\tau+(|\vec{k}+\vec{q}|-q_0)^2+\frac{\lambda\alpha}{\sqrt{r}}+\frac{3}{2}\lambda a^2+2\lambda a^2\chi(\vec{k})\right\}b^2. \tag{A4}$$

Using Eq. (7) for the self-consistent propagator and the equation of state of a uniformly ordered system, we simplify our result as

$$\delta f=\{f_B''(a)+2(|\vec{k}+\vec{q}|-q_0)^2+4\lambda a^2[\chi(\vec{k})-\chi(0)]\}b^2. \tag{A5}$$

For small r such that $q_0^2/r\gg1$ (the nearly second-order Brazovskii transition), the integral $\Pi(\vec{k})$ can be evaluated for small k as

$$\Pi(k)\approx\Pi_0[1-k^2/(4r)],\quad \Pi_0\equiv\alpha r^{-3/2}, \tag{A6}$$

which leads to

$$\chi(k)\approx\chi_0[1+\lambda\Pi_0\chi_0k^2/(8r)],\quad \chi_0\equiv(1+\lambda\Pi_0/2)^{-1}. \tag{A7}$$

In this paper, we only consider longitudinal modulations of the concentration wave amplitude, for which case we find [using Eq. (81) in Eq. (79) and comparing to Eq. (76)],

$$\mu_z(\tilde{a})=1+\frac{\tilde{a}^2}{4\tilde{r}^{5/2}[1+(1/2)\tilde{r}^{-3/2}]^2}, \tag{A8}$$

where r is implicitly a function of a and τ through Eq. (7). The mild amplitude dependence of $\mu_z(a)$ is shown in Fig. 13; $\mu_z(a)$ varies by only about 20% from the naive value $\mu_z(a)=1$ [arising from the straightforward expansion of the second term in Eq. (79)] as a varies over the relevant range. Having carefully computed this fluctuation contribution, we neglect it in the remainder of our calculations of film profiles.

However, our treatment here of the effect of fluctuations on the square-gradient coefficient has broader implications, when long-wavelength variations of the amplitude with wave vector perpendicular to the ordering directions are considered. To see this, we examine the three terms of Eq. (79) in turn. First, the term proportional to $f_B''(a)$ simply results from the fact that in a modulated state, the amplitude varies in space, so that the local free energy density becomes $f_B[a+2b\cos(\vec{k}\cdot\vec{x})]\approx f_B(a)+2b^2f_B''(a)\cos(\vec{k}\cdot\vec{x})^2$, which spatially averaged becomes $f_B(a)+f_B''(a)b^2$.

Next, if the amplitude a of the unmodulated pattern is itself small, we may evaluate the free energy to quadratic order in all the Fourier components of the concentration field, i.e., to quadratic order in both a and b. When we do that, the dependence on wave vector of the modulation comes from evaluating $(1/2)\int dq[r+(q-q_0)^2]c(q)c(-q)$, and depends only on the wave number of each Fourier component separately. In this approximation, the modulated pattern is a sum of Fourier modes each of which contributes separately to the free energy. As a result, longitudinal $(\vec{k}\|\vec{q})$ and transverse $(\vec{k}\perp\vec{q})$ modulations of *weak* patterns scale differently, since

$$(|\vec{k}+\vec{q}|-q_0)^2\approx\begin{cases}k^4/(4q_0^2), & \vec{k}\perp\vec{q}\\ k^2, & \vec{k}\|\vec{q}.\end{cases} \tag{A9}$$

This leads to thicknesses and interfacial tensions for interfaces parallel and perpendicular to the layering direction that scale differently as the transition becomes more weakly first order. This result is the origin of the claim in a recent paper by Hohenberg and Swift [28] that the interfacial tension between ordered and disordered lamellar phases is highly anisotropic, being much smaller for interfaces perpendicular to the layers (corresponding to transverse modulation of the concentration wave).

However, consider now the third term of Eq. (79), which is only present if we go beyond the quadratic order calculation, i.e., for strong initial concentration patterns. This term is $O(k^2)$ regardless of the angle between $\vec{k}$ and $\vec{q}$. Furthermore, at the first-order transition, using the scaling results Eq. (8), the coefficients $\lambda\Pi_0$, χ_0, and $a^2\lambda/r$ in the ordered state are all of order unity. By the same approach leading the Eq. (82), we can extract the square-gradient coefficient for arbitrary direction of $\vec{k}$ as

$$\mu_{\vec{k}}(a)=(\hat{k}\cdot\hat{q}_0)^2+\frac{a^2}{4r^{5/2}[1+(1/2)r^{-3/2}]^2}, \tag{A10}$$

where the second, isotropic term arises from the sum of bubble diagrams, which is the origin of the third term of Eq. (79).

In the ordered state at the transition, $\mu_{\hat{k}}(a)=0.215$ for $\vec{k}$ perpendicular to $\vec{q}$. In other words, for the uniform ordered state near the transition, the square-gradient term and hence the interfacial tension between the ordered and disordered states is only mildly anisotropic. The conclusion of Hohenberg and Swift that the nucleation droplets of lamellar phase are increasingly anisotropic for more weakly first-order transitions would appear then to be incorrect.

APPENDIX B: LINEAR RESPONSE

Recall from the main text that the linear-response results for the concentration and free energy can be written as

$$c(z)=\frac{2}{d}\sum_m \cos(\pi m z/d)g(m,0)[h_l+(-1)^m h_r], \quad \text{(B1)}$$

$$F=-\frac{A}{d}\sum_m g(m,0)[h_l+(-1)^m h_r]^2. \quad \text{(B2)}$$

Our task is to evaluate the sums appearing in Eq. (85) and (86), which we do with the use of the identity

$$\sum_k e^{-ix_k\omega}=\frac{2\pi}{\Delta}\sum_l \delta(\omega-\omega_l), \quad x_k\equiv k\Delta, \quad \omega_l\equiv\frac{2\pi l}{\Delta}. \quad \text{(B3)}$$

Here both sums are taken over all integers. This identity can be understood as follows: the set of plane waves $\{\exp(-ix_k\omega)\}$ is a complete set on the interval $\omega:(-\pi/\Delta,\pi/\Delta)$, and hence proportional to $\delta(\omega)$ on that interval. Since each summand is periodic on this interval, the entire sum must be periodic, so the sum outside the interval must be the periodic continuation of the δ function. The proportionality constant is found by integrating both sides with $\Delta/(2\pi)\int_{-\pi/\Delta}^{\pi/\Delta}d\omega\exp(ix_j\omega)$ and using orthogonality of the plane waves.

Integrating the identity Eq. (87) with $\int d\omega/(2\pi)\tilde{f}(\omega)$ [$\tilde{f}(\omega)$ denotes the Fourier transform of $f(x)$] gives

$$\sum_k f(x_k)=\frac{1}{\Delta}\sum_l \tilde{f}(\omega_l). \quad \text{(B4)}$$

Hence we may transform an infinite sum from direct space to Fourier space. For the sums of interest here, the Fourier transforms of the original summands turn out to be exponential functions, which are simple to sum.

For the linear-response profile, we have

$$c(z)=\frac{2}{d}\mathrm{Re}\left\{\sum_m (h_l e^{ik_m z}+h_r e^{ik_m(d-z)})\frac{4k_m^2}{4q_0^2 r+(k_m^2-q_0^2)^2}\right\}, \quad \text{(B5)}$$

where $k_m\equiv\pi m/d$. Note how the terms in response to the fields at $z=0$ and $z=d$ are related by the symmetry $z\to d-z$. Because the summands are even in m, we may extend the sum to negative m and divide by two (no contribution from $m=0$).

We use the following Fourier transform:

$$\int \frac{dk}{2\pi}\frac{4k^2e^{ikx}}{4q_0^2 r+(k^2-q_0^2)^2}=\xi/q_0\mathrm{Re}\{\kappa\exp(i\kappa|x|)\}. \quad \text{(B6)}$$

Here κ is the solution with positive real part to the equation

$$\kappa^2=q_0^2+2iq_0\xi^{-1}. \quad \text{(B7)}$$

Using Eq. (88) with $\Delta=2d$, we have

$$c(z)=\frac{2\xi}{q_0}\mathrm{Re}\left\{\kappa\sum_j (h_l e^{i\kappa|z+y_j|}+h_r e^{i\kappa|d-z+y_j|})\right\}, \quad y_j\equiv 2dj. \quad \text{(B8)}$$

Taking z ranging from zero to d, we can easily separate the absolute-value exponents into cases, and perform the resulting infinite geometric sums, with the final result

$$c(z)=\frac{2\xi}{q_0}\mathrm{Re}\left\{\frac{ih_l\kappa\cos\kappa(d-z)}{\sin\kappa d}+\frac{ih_r\kappa\cos\kappa z}{\sin\kappa d}\right\}. \quad \text{(B9)}$$

Now consider the sum for the linear-response free energy, Eq. (86). Expanding the factor $[h_l+(-1)^m h_r]^2=(h_l^2+h_r^2)+2(-1)^m h_l h_r$, we see that the free energy is a sum of the same form as the concentration profile at $z=0$, with $h_l\to h_l^2+h_r^2$ and $h_r\to 2h_l h_r$. Hence we read off the result as

$$F=-\frac{A\xi}{q_0}\mathrm{Re}\{i(h_l^2+h_r^2)\kappa\cot\kappa d+2ih_l h_r\kappa\csc\kappa d\}. \quad \text{(B10)}$$

[1] A. Menelle, T. P. Russell, S. H. Anastasiadis, S. K. Satija, and C. F. Majkrzak, Phys. Rev. Lett. **68**, 67 (1992).

[2] P. Lambooy, R. P. Russell, G. J. Kellogg, A. M. Mayes, P. D. Gallagher, and S. K. Satija, Phys. Rev. Lett. **72**, 2899 (1994).

[3] A. M. Mayes, T. P. Russell, P. Bassereau, S. M. Baker, and G. S. Smith, Macromolecules **27**, 749 (1994).

[4] M. D. Foster, M. Sikka, N. Singh, F. S. Bates, S. K. Satija, and C. F. Majkrzak, J. Chem. Phys. **96**, 8605 (1992).

[5] M. Sikka, N. Singh, A. Karim, F. S. Bates, S. K. Satija, and C. F. Majkrzak, Phys. Rev. Lett. **70**, 307 (1993).

[6] P.G. de Gennes, Langmuir **6**, 1448 (1990).

[7] M.S. Turner, Phys. Rev. Lett. **69**, 1788 (1992).

[8] F. Schmid and M Schick, Phys. Rev. E **48**, 1882 (1993).

[9] R. Evans, U. Marconi, and P. Tarazons, J. Chem. Phys. **84**,

2376 (1986); R. Evans, J. Phys. Condens. Matter **2**, 8089 (1990).
[10] G.H. Fredrickson and K. Binder, J. Chem. Phys. **91**, 7265 (1989).
[11] S. Brazovskii, Zh. Éksp. Teor. Fiz. **68**, 175 (1975) [Sov. Phys. JETP **41**, 85 (1975)].
[12] L. Leibler, Macromolecules **13**, 1602 (1980).
[13] G. H. Fredrickson and E. Helfand, J. Chem. Phys. **87**, 697 (1987).
[14] D. C. Morse and S. T. Milner, Phys. Rev. E **47**, 1119 (1993).
[15] T. Ohta and K. Kawasaki, Macromolecules **19**, 2621 (1986); M. Olvera de la Cruz and I. C. Sanchez, *ibid.* **19**, 2501 (1986).
[16] G. H. Fredrickson, Macromolecules **20**, 2535 (1987).
[17] K. R. Shull, Macromolecules **25**, 2122 (1992).
[18] G. Coulon, B. Collin, D. Ausserre, D. Chatenay, and T. P. Russell, J. Phys. (Paris) **51**, 2801 (1990).
[19] D. Ausserre, D. Chatenay, G. Coulon, and B. Collin, J. Phys. (Paris) **51**, 2571 (1990).
[20] N. Singh, A. Kudrle, M. Sikka, and F. S. Bates, J. Phys. (France) II **5**, 377 (1995); N. Singh (private communication).
[21] A.O. Parry and R. Evans, Phys. Rev. Lett. **64**, 439 (1990).
[22] P.-G. de Gennes and J. Prost, *The Physics of Liquid Crystals*, 2nd ed. (Clarendon, Oxford, 1993), Sec. 7.1.2.
[23] D. C. Morse and S. T. Milner (unpublished).
[24] J. W. Cahn, J. Chem. Phys. **66**, 3667 (1977).
[25] For a review, see, e.g., P.-G. de Gennes, Rev. Mod. Phys. **57**, 827 (1985); S. Dietrich, in *Phase Transitions and Critical Phenomena*, Vol. 12, edited by C. Domb and J. Lebowitz (Academic Press, London, 1988); M. Schick, in *Liquids at Interfaces*, edited by J. Charvolin, J.F. Joanny, and J. Zinn-Justin, Les Houches, Session XLVIII, 1988 (Elsevier, Amsterdam, 1990).
[26] H. Nakanishi and M. E. Fisher, J. Chem. Phys. **78**, 3279 (1983).
[27] P. Taborek and J.E. Rutledge, Phys. Rev. Lett. **68**, 2184 (1992); J.E. Rutledge and P. Taborek, *ibid.* **69**, 937 (1992).
[28] P. C. Hohenberg and J. B. Swift, Phys. Rev. E **52**, 1828 (1995).